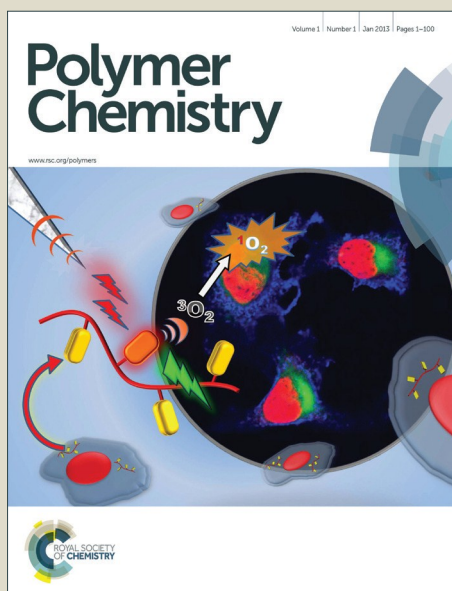


Polymer Chemistry

Accepted Manuscript



This is an *Accepted Manuscript*, which has been through the Royal Society of Chemistry peer review process and has been accepted for publication.

Accepted Manuscripts are published online shortly after acceptance, before technical editing, formatting and proof reading. Using this free service, authors can make their results available to the community, in citable form, before we publish the edited article. We will replace this *Accepted Manuscript* with the edited and formatted *Advance Article* as soon as it is available.

You can find more information about *Accepted Manuscripts* in the [Information for Authors](#).

Please note that technical editing may introduce minor changes to the text and/or graphics, which may alter content. The journal's standard [Terms & Conditions](#) and the [Ethical guidelines](#) still apply. In no event shall the Royal Society of Chemistry be held responsible for any errors or omissions in this *Accepted Manuscript* or any consequences arising from the use of any information it contains.

ARTICLE

Synthesis and Properties of Temperature-Sensitive and Chemically Crosslinkable Poly(ether-urethane) Hydrogel

Cite this: DOI: 10.1039/x0xx00000x

Received 00th January 2012,

Accepted 00th January 2012

DOI: 10.1039/x0xx00000x

www.rsc.org/Ruizhi Li,^a Na Liu,^a Bingqiang Li,^a Yinong Wang,^a Guolin Wu,^{*a} and Jianbiao Ma,^{*b}

The temperature-responsive and crosslinkable poly(ether-urethane)s (PEUs), which may be useful for the tissue adhesive, are prepared through the processes of polymerization of poly(ethylene glycol)s (PEG), Mono-p-methoxybenzylidene-pentaerythritol and hexamethylene diisocyanate, hydrolysis of the acetal in PEUs and the grafting methacrylate (MA) to PEUs. After gelating, the PEU solution in a specific temperature range via a rapid reversible temperature response, the physical hydrogel is further self-cross-linked or cross-linked with PEG diacrylate (PEGDA) by photocuring or thermal solidification. These PEU-MA gels are characterized by Fourier transform infrared spectra (FTIR), nuclear magnetic resonance (NMR) and size exclusion chromatography (SEC). The sol-gel phase transition through temperature response and chemical crosslinking are investigated by rheology testing. It is found that the swelling ratio, degradation, adhesive strength and mechanical properties of the PEU-MA gels are affected by the ratio of hydrophilic and hydrophobic segments in PEU and the grafting ratios of MA in PEU-MA gels. The adhesive strengths on the tissues with PEU-MA are stronger than glass and PBT. The adhesion on artificial duramater with PEU-MA can be kept over one month even immersed in water. The good biocompatibility of the PEU-MA gels is demonstrated via cytotoxicity evaluation. As a result, these PEU-MA gels are promising candidates to be the tissue adhesive, drug-loading materials for soft tissue filling and regeneration.

Introduction

To date, a large variety of tissue adhesives, sealants and hemostatic agents have been developed to overcome the drawbacks of conventional closure techniques (including stapling and suturing),¹ such as having a relatively long application time,^{2, 3} eliciting inflammatory responses^{4, 5} and additional damage on the tissue.¹⁻³ Thereinto, tissue adhesives are patches or glues that bind various tissues together in order to allow for the natural healing process to occur, and are applied to a variety of tissues, such as skin, intestine, subcutaneous tissue and visceral organ.⁶⁻⁸ The materials of tissue adhesives are mostly based on synthetic polymers (including polycyanoacrylates,^{9, 10} poly(ethylene glycol)s (PEGs),^{11, 12} polyurethanes¹³ and polyesters¹⁴), polysaccharide (including chitosan,¹⁵⁻¹⁷ dextran^{18, 19} and hyaluronan^{20, 21}), and protein (including fibrin²², gelatin^{23, 24} and albumin^{25, 26}).

Polyurethanes are a significant class of synthetic polymers for different tissue adhesive due to their absence of hemolytic behavior and excellent thermal stability at physiological temperature.^{1, 13} TissuGlu[®] Surgical Adhesive (Cohera Medical

Inc.) is the most prominent commercial example of polyurethanes, which is used for abdominal tissue bonding.²⁷ TissuGlu[®] is a polyurethane-based adhesive, which is a one-component glue consisting of a hyperbranched polymer with isocyanate end groups containing about 50 wt% of lysine.^{1, 27}

However, according to the feedbacks on the animal and clinical experiments,²⁸⁻³⁰ now available tissue adhesives, including cyanoacrylates (CA), polyurethanes and fibrin sealant, have been associated with limited adhesion strength, poor control over adhesion activation, or toxicity.²⁸⁻³⁰ Recently, light-activated polymers have been used to the tissue adhesives with their good properties of high adhesive strength, facilitative control over adhesion activation and biocompatibility.³¹⁻³⁵ But most of these hydrophilic adhesives were substantial swelling and quick washout in the presence of shear stress.^{28, 36}

In order to overcome the drawbacks of the photo-activated adhesives and be different from the hydrophobic light-activated adhesive (HLAA),²⁸ the temperature-sensitive³⁷⁻³⁹ and chemically crosslinkable⁴⁰ hydrogels were designed to be

used as the tissue adhesives, which were made by the poly(ether urethane)s (PEUs). Recently, many kinds of PEU have been used as biomaterials,^{41, 42} e.g., multi-responsive drug delivery systems, multi-responsive nanoparticles, and injectable hydrogels.⁴³⁻⁴⁷ For the multi-responsive PEUs, functional segments are incorporated into the backbone of PEU by a facile one-pot approach for temperature, pH and redox responses. Based on these multi-responsive PEUs, the major formation mechanism of injectable PEU gel formation is the reversible temperature-responsive physical cross-linking via hydrophobic interactions.⁴³ Nevertheless, such an injectable PEU gel was formed by a physical network and was difficult to further modify owing to the lack of groups capable of cross-linking in the PEU main chain. In this study, the temperature-sensitive and chemically crosslinkable PEU-methacrylate (MA) hydrogels are prepared through the processes of polymerization of PEG, mono-p-methoxybenzylidene-pentaerythritol (MAP) and hexamethylene diisocyanate (HDI), hydrolysis of the acetal in PEUs and the grafting MA to PEUs to form PEU-MA finally. It is possible that these PEU-MA gels might overcome the drawbacks of the photo-activated adhesives mentioned above. Firstly, the temperature of reversible sol-to-gel transition of PEU-MA solution is 34 °C, below the physiological temperature, so the PEU-MA solution can be gelled rapidly after it contacted with the body. It is prevented that the gels could be washed out in the presence of shear stress. Moreover, these reversible gels could be further photocured to form the low-swelling gels, of which the minimum swelling ratio was only 0.5. It is avoided the substantial swelling of the photocured gels. The functional drugs could be also loaded in the PEU-MA gels to achieve the outcome of anti-inflammatory and analgesia when the PEU gels are used to the adhesive of subcutaneous tissue or visceral organ.

Experimental Details

Chemicals and reagents

2-Hydroxy-4'-(2-hydroxyethoxy)-2-methylpropiophenone (I2959) (98%), triethylamine (TEA) (99%), 2,2'-azobis(2-methylpropiionamide) dihydrochloride (AIBA) (98%) and poly(ethylene glycol) diacrylate (PEGDA) (99%, Mw = 600) were purchased from J&K Scientific Ltd. (Beijing, China). PEG (Mw = 1000, 1500, and 2000 Da), HDI (98%), anisaldehyde (99%), pentaerythritol (99%) and methacryloyl chloride (MAC) (99.5%) were obtained from Sigma-Aldrich (Shanghai, China).

Instruments and Measurements

Nuclear magnetic resonance (NMR) measurements of the ¹H-NMR and ¹³C-NMR spectra were recorded at room temperature by a Bruker AC-400 NMR spectrometer using CDCl₃ or DMSO-*d*₆ as the solvent, and tetramethylsilane as the internal standard. Fourier transform infrared spectra (FTIR) were measured with a Bio-Rad FTS6000 spectrophotometer at room temperature. The samples were prepared by well-dispersing the

complexes in KBr powder and compressing the mixtures to form a plate. The molecular weight and distribution of the polymers were determined by size exclusion chromatography (SEC, Waters 2414 system Milford, MA) at 35 °C. Tetrahydrofuran (THF) was used as the eluent at a flow rate of 1.0 mL·min⁻¹. The average weights were calibrated with standard polystyrene samples.

The sol-gel phase transition was measured by the inverting test with a 2 mL (10 mm diameter) via test tube at temperature intervals of 2 °C.⁴³ A series of PEU solutions (of given concentrations in 0.01 M PBS buffer solution (pH 7.4)) were preserved at 5 °C for 24 h. The sol-gel phase transition behaviour of the sample at each concentration was measured by inverting the vial after keeping it at a constant temperature for 15 min. It is defined as a gel state if no fluidity is visually observed by inverting the vials for 1 min, or a sol state if it flows.⁴³ After testing, temperature was reverted to the original low temperature range to observe the reversibility of the PEU solutions. Tensile and adhesion tests were performed by Testometric M500-25kN (Testometric Company Ltd, Rochdale, England) at room temperature, for the studies of adhesion (MPa), stress at break (MPa), strain at break (%), and Young's modulus (MPa)⁴⁸. All the samples were strained at 200 mm min⁻¹.

Synthesis of MAP

MAP was prepared according to a minorly modified procedure.⁴⁹ Briefly, pentaerythritol (13.6 g, 0.1 mol) was dissolved in deionized water (100 mL). And then stirring was started and concentrated hydrochloric acid (0.5 mL) was added, followed by p-anisaldehyde (1.35 mL, 11.1 mmol). When the precipitate of MAP started forming, dropwise addition of p-anisaldehyde (11.5 mL, 94.7 mmol) was begun. After the addition of p-anisaldehyde was completed, the mixture was stirred for additional 4 h. The precipitate was collected and washed with diluted Na₂CO₃ aqueous solution and ethyl ether. The solid was dried under vacuum over phosphorus pentoxide to give MAP as a white solid (22.3 g, 87%).

MAP (¹H-NMR, CDCl₃, 400 MHz, Fig. S1): δ 3.23-3.24 (d, 2H), 3.66-3.67 (d, 2H), 3.74 (s, 3H), 3.77 (d, 2H), 3.87-3.90 (d, 2H), 4.50 (t, 1H), 4.58 (t, 1H), 5.34 (s, 1H), 6.89-6.91 (d, 2H), 7.31-7.33 (d, 2H). (¹³C-NMR, CDCl₃, 400 MHz, Fig. S2): δ 39.46 (C-CH₂), 55.53, 60.09 and 61.57 (CH₂O), 69.54 (CH₂OH), 101.1 (O-CH₂-O), 113.72, 127.92 and 131.73 (CH=CH-CH=CH), 159.83 (O-CH=CH). IR (neat, KBr, cm⁻¹, Fig. S3): ν(O-H) 3250, (C-O) 1110, (C-H in benzene ring) 800, 660. Mp: 164-166 °C. Anal. Calcd for C₁₃H₁₈O₅: C, 61.42; H, 7.09. Found: C, 61.38; H, 7.13.

Synthesis of PEU-MAP

The PEU copolymers were prepared according to a minorly modified procedure.⁴³ Briefly, a series of random PEU copolymers were synthesized by a one-pot polyaddition of PEG, MAP, and HDI. The polyaddition was conducted at specified molar ratios (as shown in Table 1). The specific

reaction procedure is as follows: a solution of specified amounts of PEG and MAP in mixed solution with 1,2-dichloroethane and THF (v/v=1:1) was prepared. Then, a solution of a specified amount of HDI in 1, 2-dichloroethane was prepared with a catalytic amount of dibutyltin dilaurate (0.5 wt%, with respect to the reactant), and added dropwise to the (PEG+MAP) solution such that the molar ratio of HDI to (PEG+MAP) was 1:1. Finally, the reaction mixture was stirred at 80 °C under a dry nitrogen atmosphere for 24 h. After the procedure, an excess of methanol was added, and the mixture was reacted for an additional hour to eliminate any remaining dibutyltin dilaurate or oligomer residue. The resulting products were collected by precipitation in diethyl ether, and then collected through filtration, and followed by drying under vacuum until a constant weight was reached, affording a yield of over 90%.

Synthesis of PEU-Methacrylate (PEU-MA)

The hydrolysis of the acetal portions in PEU-MAP was followed by the next procedure. Briefly, the obtained PEU-MAP copolymers (4.0 g) were dissolved in H₂O/THF mixed solutions (200 mL, v/v = 1:1), and then concentrated hydrochloric acid was added under stirring at pH 3.0 for 12 h. After hydrolysis, the solution was neutralized by NaOH to pH 7.0. And then the unnecessary THF, anisaldehyde and NaCl were removed by a dialysis membrane (MWCO, 3.5 kDa) in deionized water. The hydrolysed PEU was obtained by freeze-drying, affording a yield of over 72%.

The olefination of hydrolysed PEU was followed by the next procedure. Briefly, the hydrolysed PEU (2.0 g) was dissolved in dry CH₂Cl₂ (100 mL) with TEA as an acid-binding agent. The specified amount of MAC was dissolved in dry CH₂Cl₂. And then the MAC solution was added dropwise to the PEU solution at 0 °C under a dry nitrogen atmosphere for 12 h. After olefination, the reaction system was washed by saturated Na₂CO₃/NaCl aqueous solution. The resulting products were collected by precipitation in diethyl ether, and then collected through filtration, and followed by drying under vacuum at room temperature until a constant weight was reached, affording a yield of over 85%.

Preparation of Photocured PEU-MA and PEU-MA-PEGDA Hydrogels and Gel Membranes

PEU-MA or PEU-MA-PEGDA hydrogels were formed by mixing a specified amount of PEU-MA or PEU-MA with PEGDA in deionized water, respectively, with 0.1 wt% I2959 as a photoinitiator. The molar rate of PEGDA to MA in PEU was 1:2. The cross-linking reaction was initiated by exposure to UV light (ca. 5 mW·cm⁻², model 100AP, Blak-Ray) for 2 min. The hydrogels obtained by UV solidification were dried under vacuum at 50 °C until a constant weight was reached. The hydrogels were then used to form membranes for the swelling ratio tests, *in vitro* and *in vivo* degradation, and the tensile tests.

Rheology Test

The rheology properties of the hydrogels were tested by an AR2000ex rheometer (TA Instruments). Temperature-dependent changes in the elastic modulus (G') and the viscous modulus (G'') were recorded by an aluminium parallel plate with a diameter of 40 mm. The sample gap was set to 1.0 mm. The temperature was controlled by a Peltier system with the bottom plate connected to a water bath. The rheology tests consisted of two samples. Sample 1 was prepared by mixing PEU2000-MA (0.5 g) in the PBS buffer solution (2.5 mL, pH 7.4). The frequency was 1 rad·s⁻¹, with a target strain value of 10%. The temperature was increased from 15 to 40 °C at a warming rate of 2 °C·min⁻¹. And then, the temperature was decrease from 40 to 15 °C at a cooling rate of -2 °C·min⁻¹. After testing, Sample 1 was removed. Sample 2 was added on the plate, which was prepared by mixing PEU2000-MA (0.5 g) and PEGDA (0.1 g) as the cross-linking agent in the PBS buffer solution (2.5 mL, pH 7.4), with AIBA (0.1 wt%) acting as a thermal initiator. The plate was heated from 15 to 70 °C at a heating rate of 1 °C·min⁻¹ and cooled from 70 to 15 °C at a cooling rate of -1 °C·min⁻¹. In addition, Sample 2 was used to determine the kinetics of the chemical cross-linking at 35, 50 and 60 °C.

Swelling Ratio Test

The swelling ratio measurement was conducted by soaking the dried samples in a temperature-controlled bath of deionized water. The temperature of the water bath was adjusted individually to 20, 25, 30, 33, 35, 37, 40, 45, and 50 °C. After 12 h of soaking, the samples were taken out from the water bath and gently blotted with filter paper to remove surface water, followed by immediate weighing. The swelling ratio (SR) was calculated according to the following equation:

$$SR = (W - W_0) / W_0$$

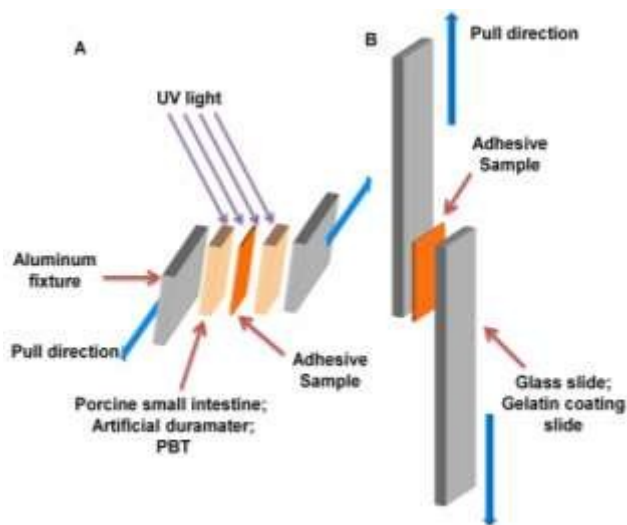
, where W_0 and W denote the weights of the dried and swollen samples, respectively.

In Vitro Degradation

Degradation rates were measured by incubating dried PEU-MA or PEU-MA-PEGDA hydrogels in 20 mL of 10 mM PBS buffer solution at pH levels of 7.4, 9.0, and 4.0 under continuous shaking (60 strokes·min⁻¹) at 37°C. The same tests were performed with a 0.1 M ascorbic acid/sodium ascorbate (AH₂/AH⁻) buffer solution at pH 4.0 and a pH 7.4 PBS buffer solution with lipase. The specific processes of this two tests were that 2000 units of lipase per day (100 units·mL⁻¹) were added to the pH 7.4 PBS buffer solution, and 0.2 mL of 3 wt% H₂O₂ per day (reactive oxygen species (ROS)) were added to the AH₂/AH⁻ buffer solution in the first 5 days. After testing, the samples were the removed, washed in deionized water, dried under vacuum at 50 °C for 4 days, and weighed again to determine the mass loss.

In Vivo Mass Decrease of Gel Membranes

All animal experiments were conducted in accordance with the Management Ordinance of Experimental Animal of China ([2001] No. 545) and were approved by the Tianjin City according to the experimental animals management rules ([2004] No. 30). For measurements of *in vivo* gel membranes mass decrease,⁵⁰ the male Sprague-Dawley (SD) rats ($n = 3$) were used as model animals. Several uniform fragments of dried PEU-MA gel membranes mentioned above were weighed, immersed in PBS (pH 7.4) to swelling equilibrium, and then implanted in the SD rats' subcutaneous tissues after autoclaving. After each time interval, the residual gel membranes were separated from skin, dried under vacuum at 50 °C until a constant weight was reached, and then weighed for determination of time-dependent gel membranes mass decrease.



Scheme 1. Schematic illustration of lap shear testing using porcine small intestine, artificial duramater and PBT after pre-activating the PEU-MA and PEU-MA-PEGDA (A), glass slide and gelatin coating slide (B).

Adhesive Strength Test

The measurement of adhesive strength of the PEU-MA and PEU-MA-PEGDA gels were performed by lap shear testing.⁵¹ The Compant[®] Medical Adhesive (made by cyanoacrylate (CA), Aoke Health Medical Equipment Ltd.), PEU-MA and PEU-MA-PEGDA solutions were coated to the transparent glass slide (or gelatin coating slide, width of 1.5 cm); another glass slide was placed on the top of the original slide; and then the two slides were exposure to UV light to activate the PEU-MA and PEU-MA-PEGDA for 2 min. The adhered slides were used to measure the adhesive strength (as shown in Scheme 1B). In order to measure the adhesive strength of the PEU-MA and PEU-MA-PEGDA on the tissue, the gelatin coating slide, porcine small intestine and artificial duramater (made by porcine pericardium, Grandhope Biotech Ltd.) were used as the samples. The porcine small intestine or artificial duramater was glued onto two flat aluminous substrates (width of 1 cm); and the patches coated with the PEU-MA or PEU-MA-PEGDA solution were exposure to UV light directly to pre-activate the PEU-MA gels for 1 min at 37 °C as the UV light is difficult to

penetrate through the aluminous substrate. And then the two tissue-attached aluminous fixtures were adhered together when the UV light irradiating from the side for 1 min and then from the other side for another 1 min (As shown in Scheme 1A). The polybutylene terephthalate (PBT) was also used as the sample to measure the adhesive strength under the conditions mentioned above (Scheme 1A). Several patches of artificial duramater adhered with PEU2000-100MA were immersed in PBS at pH 7.4, 37 °C, and the adhesive strengths were measured at the time points of 7, 14 and 28 days. The strain rate was 200 mm·min⁻¹ at 25 °C.

In Vitro Drug Release

Ibuprofen was selected as a model drug for the drug release of PEU hydrogels. Ibuprofen was first dissolved in a PBS solution with a concentration of 50 g·L⁻¹. Second, 50 mg PEU-MA or 50 mg PEU-MA with 10 mg PEGDA were added into 0.50 mL of prepared ibuprofen solution, respectively. As a result, drug containing PEU solutions with concentrations of 10% were prepared. Third, I2959 (0.1 wt%) was added into this two PEU solutions, and then they were exposure to UV light (ca. 5 mW·cm⁻²) for 2 min at 37 °C until the cross-linking reaction was completed to obtain drug-loaded hydrogels.

The obtained ibuprofen-loaded hydrogels (0.10 g) were sealed in dialysis membrane tubes (MWCO, 3.5 kDa) and immersed in 20 mL of PBS buffer at pH 7.4. The mixtures were shaken at 37 °C. At predetermined intervals, 3 mL of release medium was collected for testing and replaced by an equal volume of fresh buffer. The concentration of released ibuprofen from hydrogels was quantified by an UV spectrophotometer (Shimadzu Co. Japan) at 263 nm. The cumulative ibuprofen release was calculated as:

$$\text{Cumulative release (\%)} = (V_e \sum_{i=1}^{n-1} C_i + V_0 C_n) / m_{\text{drug}} \times 100$$

, where V_e is the amount of release media took out every time, V_0 is the amount of release medium, C_i is the concentration of ibuprofen released from hydrogel at displacement time of i , m_{drug} is the mass of drug used for release, and n is the displacement time. Three replicates were measured for each sample, and the results presented are the average data.⁵²⁻⁵⁴

Cell Culture Studies

The cytotoxicity of PEU-MA and PEU-MA-PEGDA gels was evaluated with NCTC clone 929 (L-929) cells. L929 cells were cultured in Dulbecco Modified Eagle Medium (DMEM) with 1% penicillin-streptomycin and 10% FBS in cell flasks. The L-929 cells were incubated at 37 °C under a humidified atmosphere with 5% CO₂ for 3 days. The PEU-MA or PEU-MA-PEGDA solutions were added into a 96-well tissue culture plate and exposure to UV light (ca. 5 mW·cm⁻²) for 10 min at 37 °C to solidify and sterilize the gels in the clean bench. The L-929 cells grown in cell flasks were then detached on confluency by

adding 1 mL 0.25% trypsin with 0.1% EDTA. The cells were seeded on the top of the gels at a density of 1×10^5 cells per well, and incubated to support cell growth.

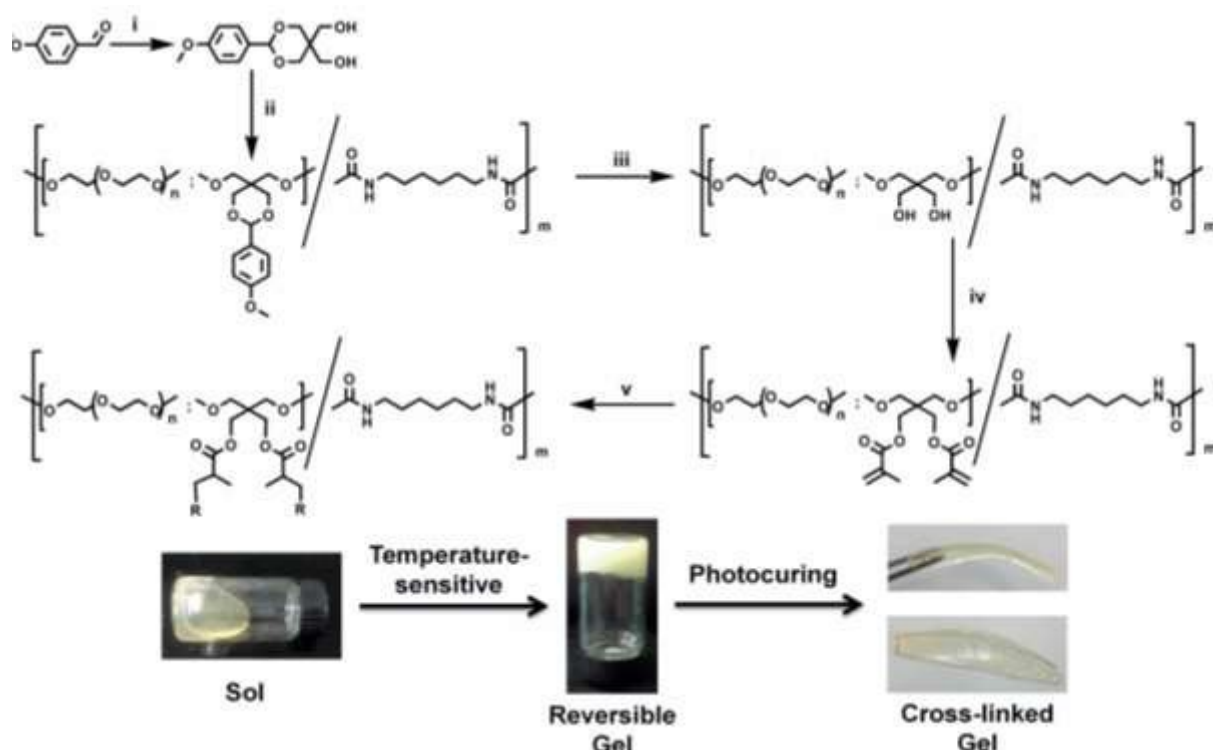
After incubated at 37 °C under 5% CO₂ for 12, 24 and 48 h, AO/EB was added into the 96-well culture plate to stain the L-929 cells. The cells were then incubated for 1 h, and observed by an inverted microscope.

MTT assay was also used to investigate the biocompatibility of PEU-MA and PEU-MA-PEGDA gels. After time points of 24 and 48h, 100 μL of MTT solution (5 mg·mL⁻¹) was added into the well plate and incubated for a further 4 h. The solution of MTT was removed and 150 μL DMSO were added to each well to dissolve the formazan crystals of the MTT. The

absorbance of each well was measured by a microplate reader (Labsystem, Multiskan, Ascent, Model 354 Finland) at 490 nm. The relative cell viability was defined by comparing them with the absorbance of the control wells, which only contained cell culture medium at 490 nm. The cell viability was calculated according to the following equation:

$$\text{Cell viability (\%)} = (A_s / A_c) \times 100\%$$

, where A_s is the sample absorbance at 490 nm, and A_c is the absorbance at 490 nm of the positive control. Cells incubated in the absence of the gels in the DMEM complete medium were used as this positive control.



Scheme 2. Synthetic routes of MAP, random PEU-MAP copolymers and PEU-MA hydrogels. Reagents and conditions: (i) pentaerythritol, concentrated HCl, rt; (ii) PEG, HDI, 1,2-dichloroethane, dibutyltindindiluarat, N₂ atmosphere, 80 °C, 24h; (iii) THF, water, concentrated HCl, rt; (iv) CH₂Cl₂, MAC, 0 °C; (v) No cross-linking agents or PEGDA; I2959, *hv*. R: PEU-MA or PEGDA-MA-PEU.

Table 1. Summary of the synthetic random PEU copolymers

Polymer	Mw/Da (PEG)	PEG:MAP (n/n)	Mn/Da	Mw/Da	Dispersity	Solubility in H ₂ O at 25°C
PEU1000-MAP	1000	1:1.5	24413	60544	2.48	Sol.
PEU1000-MA	1000	1:1.5	20543	39443	1.92	Sol.
PEU1500-MAP	1500	1:3	23617	51013	2.16	Sol.
PEU1500-MA	1500	1:3	18643	32066	1.72	Sol.
PEU2000-MAP	2000	1:4	26518	63908	2.41	Sol.
PEU2000-MA	2000	1:4	22487	46548	2.07	Sol.

Results and Discussion

The purpose of this work is to develop a temperature-sensitive PEU hydrogel capable of chemically cross-linking. Such a

hydrogel would be a promising candidate for tissue adhesive and drug-loading hydrogel, which may be applied in the field of tissue engineering.

The design of the hydrogel was based on the guidelines below: firstly, MAP was synthesised by the condensation

reaction with pentaerythritol and p-anisaldehyde. Secondly, equal amounts of HDI and diols of MAP and PEG were used to prepare random PEU copolymers via a one-pot additional polymerization. Finally, the acetal moieties in the PEU were hydrolysed and the MA was grafted to the PEU main chain. The MA and HDI moieties of the copolymers comprise the hydrophobic parts of the solution. The olefin groups of the MA serve as the points of chemical cross-linking in the copolymers. The PEG moieties serve as the hydrophilic segments. The solution of PEU copolymers in PBS at pH 7.4 undergoes a reversible and rapid sol-gel transition with increasing temperature. After the gelation of the PEU-MA solution at the specified temperature range, the physical hydrogel can be further self-cross-linked or cross-linked with PEGDA by UV curing or thermal initiation. The cured PEU-MA hydrogels can maintain the gel state and shape across a wide temperature range including when the temperature is reverted to the original solution temperature range. The further cross-linking time of the PEU-MA is around 2 minutes for UV curing and not more than 30 minutes for thermally initiating.

the C=O and N-H stretching of the urethane groups, respectively. The disappearance of the absorption peak of the isocyanate group near 2272 cm^{-1} (Fig. 1B) in the FTIR spectra of the PEU2000-MA copolymers and the PEU2000-MA gels (Fig. 1A and C) indicates that no unreacted isocyanate groups remain in the resulting copolymer and gel. The $^1\text{H-NMR}$ spectrum of PEU2000-MA is shown in Fig. 2, which indicates the coexistence of MA, PEG, hexamethylenediamine (HDA) and remaining MAP in the copolymer. SEC measurements were performed to determine the molecular weights and polydispersity indices of the synthesized copolymers (Fig. S7). The SEC characterization results for all of the synthesized multiblock PEU copolymers (PEU1000, PEU1500, PEU2000 and their MA) are summarized in Table 1. The molar ratios of PEG to MAP in, PEU1000 and PEU1500 are maintained due to their solubility in water and the approximately constant molar ratio between the hydrophilic portions (structural units of $\text{CH}_2\text{CH}_2\text{O}$ in PEG) and the hydrophobic portions in PEU2000 (HDA and MAP parts), which is caused by the temperature-sensitive hydrogels formed by PEU2000-MA.

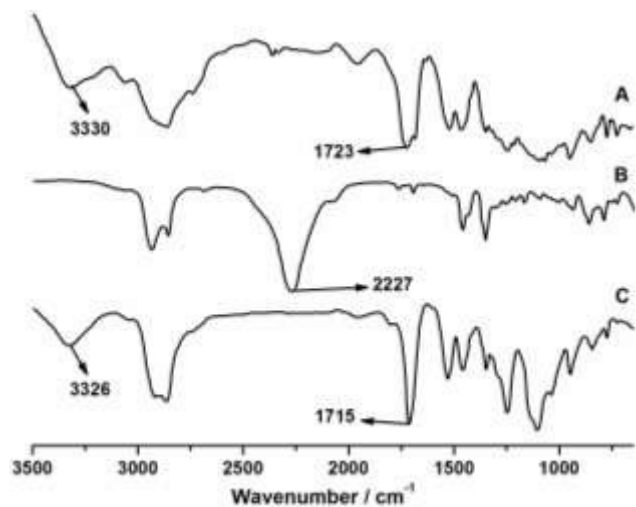


Figure 1. FT-IR spectra of photocured PEU2000-MA gels (A), HDI (B) and PEU2000-MA (C).

The synthetic route of PEU-MA hydrogel formation is illustrated in Scheme 1. The first step was to synthesis the MAP, and the product was characterized by $^1\text{H-NMR}$, $^{13}\text{C-NMR}$ and FTIR (Fig. S1, S2 and S3). The second step was the synthesis of the PEU copolymer with MAP, HDI and PEG. The third step was the hydrolysis of the PEU acetal portions and the olefination of the hydrolysed PEU to obtain PEU-MA. Finally, the cross-linked PEU-MA or PEU-MA-PEGDA hydrogels were prepared by UV-curing after the physical PEU hydrogel network had formed. The intermediate products of PEU-MAP and hydrolysed PEU were characterized by $^1\text{H-NMR}$ and FTIR (Fig. S4-6). Figure 1 shows the FTIR spectra of the photocured PEU2000-MA gels (A), HDI (B), and PEU2000-MA copolymers (C). The FTIR spectra of the PEU2000-MA copolymers and the PEU2000-MA gels share common absorption peaks near 1715 and 3330 cm^{-1} that are assigned to

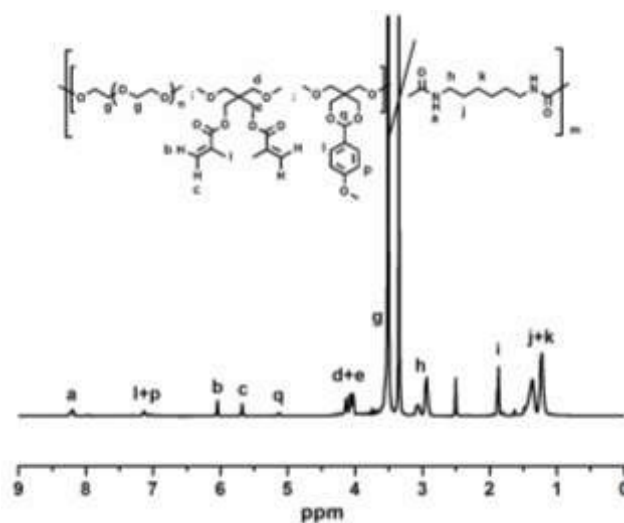


Figure 2. $^1\text{H-NMR}$ spectrum of PEU2000-MA in $\text{DMSO-}d_6$.

Hydrolysis of Acetal Portions in PEU. The kinetics of acetal hydrolyses was measured as follow. The acetal portions in PEU were hydrolysed at different pH and detected by UV/vis spectroscopy by measuring the absorbance at 279 nm .⁵⁵ The PEU-MAP (0.2 g) was dissolved in phosphate buffer solution (PBS, 100 mL, pH 7.4) and PBS/THF mixed solution (50 mL of PBS and 50 mL of THF, pH 7.4), respectively. The prepared PEU aqueous solution and PEU solution of PBS/THF were divided into four aliquots and adjusted to pH 3.0, 4.0, 5.0, and 7.4, respectively, by addition of 50 μL of 4.0 M pH 3.0, 4.0, and 5.0 acetate buffers or pH 7.4 phosphate buffer, while keeping the same of the salt concentration. All of the samples were shaken at $37\text{ }^\circ\text{C}$. At the expected time points, 50 μL aliquots were removed and diluted with 2.95 mL phosphate buffer (0.1 M, pH 7.4) and the absorbance at 279 nm was measured. Finally, all the samples were completely hydrolysed

by addition of 1.0 mL concentrated HCl for excess 1 h and were measured again to determine the absorbance at 100% hydrolysis, which was used to calculate extent of acetal hydrolysis. The degree of complete hydrolysis (DH) of the PEU-MAP which was finally hydrolysed by concentrated HCl was determined by ^1H NMR (Fig. S5).⁵⁶

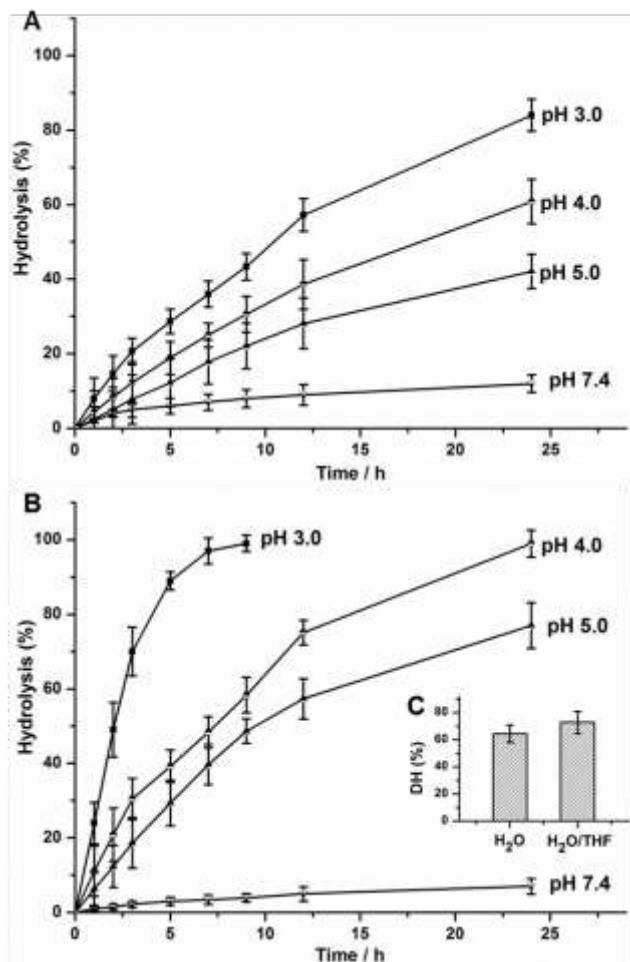


Figure 3. Kinetics of hydrolysis of the PEU acetal portions in Water (A) and in THF/Water mixed solvent (B) and the degree of complete hydrolysis (DH) (C).

The kinetics of acetal hydrolysis and DH were shown in Fig. 3. As shown in Fig. 3A or 3B, the hydrolysis rate was relative to the pH value of the solution. The low pH value could accelerate the hydrolysis of the acetal. The results showed that the hydrolysis rate of the acetals in PBS/THF mixed solutions were faster than in PBS (Fig. 3A and 3B).

While negligible hydrolysis was observed after 24 h at pH 7.4 both in the PBS/THF mixed solutions and PBS, rapid hydrolysis took place at pH 3.0 and 4.0, with half-lives of 2 and 7 h in mixed solutions, and half-lives of 7 and 9 h in PBS, respectively. The hydrolysis degree at 24 h was 42.1% in PBS and 77% in mixed solutions at pH 5.0. The rates of hydrolysis in PBS were similar to those reported by Zhong et al. for PEG-Polycarbonate copolymers with p-methoxybenzylidene acetals attached at the side.⁵⁵ And the DHs of PEU2000-MAP were 64.5% in PBS and 72.8% in mixed solutions (Fig. 3C). The

reason of these phenomena is that the acetal (MAP) and HDA portions in PEU are reunited to form the hydrophobic cores in PBS. The acetals wrapped in the hydrophobic cores are difficult to contact with H₂O and the hydrogen ion. Nevertheless, THF is a good solvent for MAP and HDA. The addition of THF in solvent can help the stretch of the segments in the hydrophobic cores, which induce more H₂O and the hydrogen ion could be diffused into the core and accelerate the hydrolysis. Moreover, the grafting ratios of MA are relative to the degree of complete hydrolysis, which are also determined by ^1H NMR (Fig. 2).⁵⁶ In this study, the mentioned “PEU2000-56MA” means that the grafting ratio of MA in PEU2000 is 56%.

Rheology Properties. The transition behaviour from the sol to the gel state occurred abruptly, and could happen within 10 s. The purpose of the testing of rheological properties is to observe the capability of rapidly gelating and keeping gel state. Variations of G' and G'' of the PEU2000-100MA solutions (Fig. 4) were detected as a function of temperature with dynamic rheological analysis. As shown in Fig. 4A and 4B, the PEU2000-100MA solution has a Lower Critical Solution Temperature (LCST) from sol state to gel state. In the warming process, the LCST of this solution is 34 °C, and in the cooling process, the gel could convert to sol state also at 34 °C, reversibly. Oddly, if the temperature was increased higher than 60 °C, this originally reversible hydrogel is difficult to convert to sol state when the temperature was decreased to 15 °C without any excess initiator (Fig. S8). This phenomenon might be caused by the radical polymerization of the MA, which is initiated by the trace amounts of reactive oxygen species (ROS) in water.⁵⁷⁻⁵⁹ Figure 4C showed a warming and cooling procedure with the sample of PEG2000-100MA, PEGDA as a cross-linking agent and AIBA as an initiator. Once the cross-linking reaction has happened, the gel formed by the temperature-sensitive is not reversible. The PEU2000-100MA-PEGDA hydrogel could well keep the gel state even when the temperature was decreased to 15 °C. Interestingly, other PEU-MA copolymers (such as PEU1000-MA and PEU1500-MA, even PEU2000-56MA and PEU2000-21MA) cannot form the reversible and temperature-sensitive hydrogels below 40 °C except PEU2000-100MA (Fig. S9 and S10). The reversible hydrogel of PEU2000-100MA might be formed by the enough strong of hydrophobic interaction and hydrogen-bonding interaction. The kinetics of the PEU2000-100MA-PEGDA chemical cross-linking at 35, 50, and 60 °C (at which temperatures the PEU2000-100MA solution was in the gel state) was also determined by dynamic rheological analysis. As shown in Fig. 4D, the PEU2000-100MA solutions gelled within 10 s at each test temperature, and the values of the G' and G'' of PEU-MA at 35 °C were nearly constant because the initiator (AIBA) only decomposes with difficulty at this temperature. As the decomposition rate of the initiator increases with temperature, the cross-linking rate of the PEU-MA with PEGDA at 60 °C was the fastest of the three test temperatures. The rate of chemical cross-linking was closely related to the decomposition rate of the initiator.

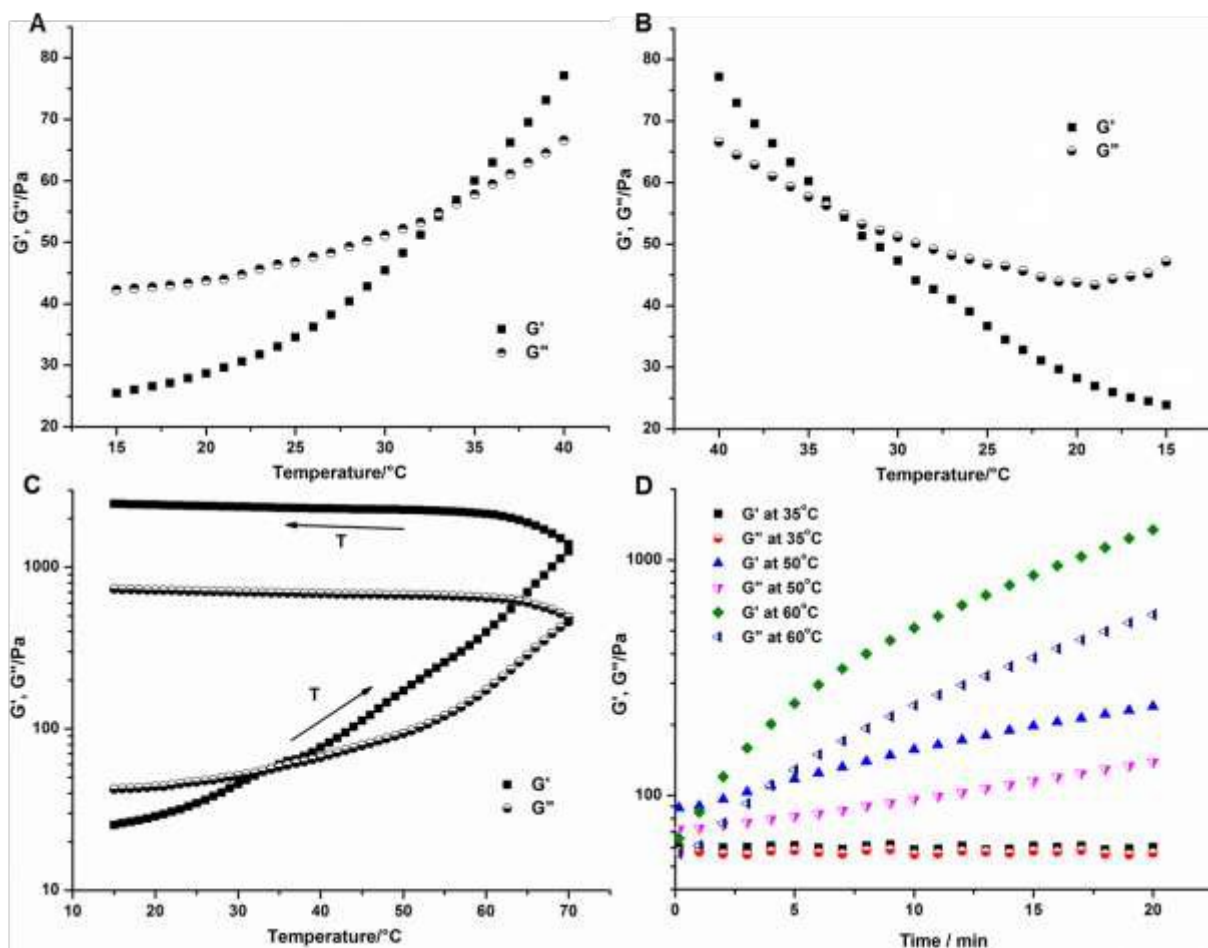


Figure 4. Rheology tests of PEU2000-100MA aqueous solution: (A) 20 wt% PEU2000-100MA solutions at warming process from 15 to 40 °C; (B) 20 wt% PEU-100MA solutions at cooling process from 40 to 15 °C; (C) 20 wt% PEU2000-100MA and 5 wt% PEGDA solutions with 0.1% AIBA as initiator at warming (from 15 to 70 °C) and then cooling (from 70 to 15 °C) processes; and (D) kinetics of chemical cross-linking of PEU2000-100MA-PEGDA solutions with 0.1% AIBA as initiator at 35, 50, 60 °C.

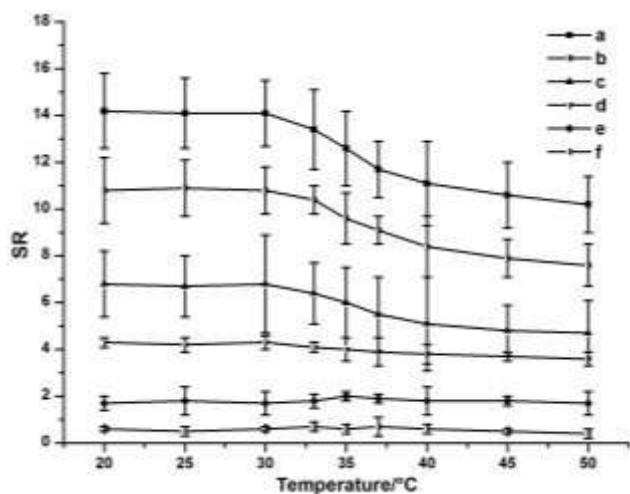


Figure 5. Swelling ratios of photocured PEU2000-56MA-PEGDA (a), PEU2000-100MA-PEGDA (b), PEU2000-56MA (c), PEU2000-100MA (d), PEU1500-100MA (e) and PEU1000-100MA (f) gels in PBS at different temperatures.

Swelling Test. The favourable property of hydrogels is their ability to swell but not dissolve in a solvent due to their chemically or physically cross-linked network. An appropriate swelling value is one of the basic requirements for hydrogels used in biomedical and tissue engineering. The swelling value is correlated with the gel cross-linking density, which is influenced by the content of MA in the copolymer. The equilibrium swelling value will usually increase with decreasing cross-linking density. Therefore, the swelling value is always used to qualitatively characterize the cross-linking density of the hydrogels.^{21, 60-62}

The effects of PEG segment length in PEU, the content of MA and temperature-to-swelling ratio of the photocured PEU-MA and PEG2000-MA-PEGDA hydrogels were studied. The grafting ratio of MA moieties in the PEUs can be obtained by calculating the peak area ratio via the ¹H-NMR spectrum of PEU-MA (Fig. 2). As shown in Fig. 5, the low grafting ratio of MA in the PEU2000-MA gels results in high swelling ratios, because the gel network formations are tight when the grafting ratio of MA is high. The swelling ratios of the PEU-100MA

gels are nearly temperature independent, and the swelling ratio increases from PEU1000-100MA to PEU2000-100MA.

PEU2000-MA-PEGDA, because the polymethacrylate (PMA) chain might appear in the PEU2000-MA gels.

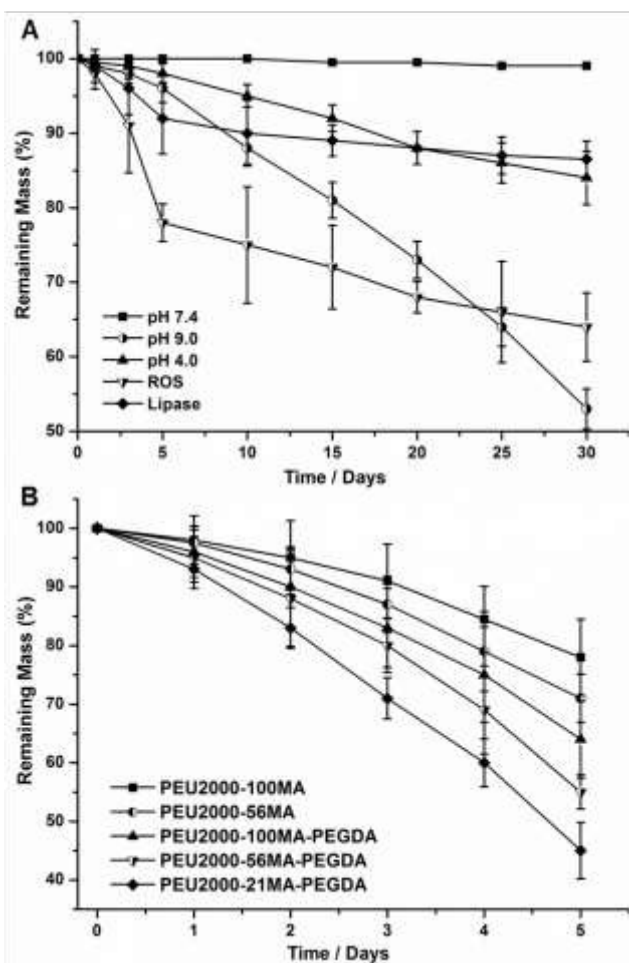


Figure 6. *In vitro* degradation of photocured PEU2000-100MA gels (A) and PEU2000-MA or PEU2000-MA-PEGDA gels degraded by ROS (B).

These phenomena are related to the hydrophilicity and uniformity of the cross-linking point in the PEUs. The short PEG segments in the PEUs decrease the hydrophilicity of the PEU-100MA hydrogels, but increase the uniformity of the cross-linking points in the PEUs. This is due to the lack of cross-linking groups contained in the PEG segment, and leads to a tighter gel cross-linked network. As the grafting ratio of MA moieties in the PEU2000-100MA gel decreases, the influence of temperature on the swelling ratio becomes apparent, as a result of the dehydration of the PEG segment that occurs at high temperatures. However, when the grafting ratio of MA moieties in the gels is increased, the segmental motion of the PEU2000 is blocked by the rigid cross-linked network, which leads to a weakening the influence of temperature on the swelling ratio of PEU2000-100MA.

Moreover, the swelling ratios of PEU2000-MA-PEGDA gels are higher than the PEU2000-MA gels at the same grafting ratio of MA moieties. These phenomena might indicate that the gel network formations of the PEU2000-MA are tighter than the

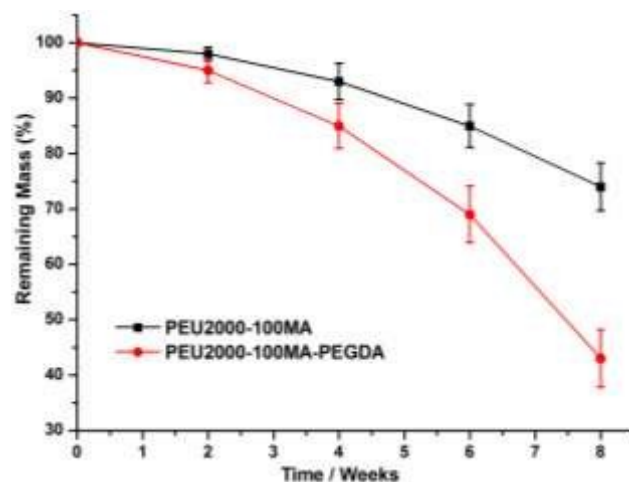


Figure 7. *In vivo* mass decreases of photocured PEU2000-100MA and PEU2000-100MA-PEGDA gel membranes.

***In Vitro* Degradation.** As shown in Table 1, all of the molecular weights and dispersities of PEU-MA are lower than the PEU-MAP. This phenomenon might indicate that the PEU copolymers could be hydrolysed under the acid condition when the acetal hydrolysis was happened. In order to verify this inference and study the biodegradability of each PEU-MA hydrogels, the degradation tests of PEU hydrogels were conducted under various environments at 37 °C including: physiologically neutral (pH 7.4), weakly acidic (pH 4.0), weakly alkaline (pH 9.0), reactive oxygen species (ROS), and lipase (pH 7.4). ROS represents a class of significant oxygen radicals, including $O_2^{\cdot-}$, H_2O_2 , and $\cdot OH$.⁵⁷⁻⁵⁹ The species in this class with the highest activity is the hydroxyl radical ($\cdot OH$).⁵⁸ The ROS could be released by adherent macrophages and foreign body giant cells (FBGCs) *in vivo*.⁶³⁻⁶⁶ The release rate of the ROS is 0.55-0.65 $nmol \cdot min^{-1}$ per 1×10^7 cells from leukocytes under inflammation.⁶⁷ It has been demonstrated that the PEU could be degraded by ROS.⁶⁵ In this study, the improved Fenton reagents composed of ascorbic acid and H_2O_2 were used to simulate the ROS environment *in vitro*.⁶⁸⁻⁷⁰ The $\cdot OH$ produced by the improved Fenton reagents were used to degrade the PEU-MA hydrogel.⁷⁰

As shown in Fig. 6A, although the PEU1000-100MA (Fig. S11) and PEU2000-100MA hydrogels experienced little degradation after 30 days of exposure at pH 7.4, the degradations of PEU1000-100MA (95.5% of remaining mass) and PEU2000-100MA (91.5% of remaining mass) were relatively obvious under the same conditions for 80 days (Fig. S12). The remaining mass of PEU1000-100MA after 30 days at pH 4.0 and 9.0 was 92% and 68%, respectively. Similarly, the remaining mass of PEU2000-100MA after 30 days at pH 4.0 and 9.0 was 84% and 53%, respectively. The H_2O_2 and lipase were continuously added to the degradation system over the first 5 days, and as a result the degradation rate over the first 5 days was faster than over the last 25 days. When the lipase

addition ceased, the PEU-MA hydrogels were difficult to degrade. This is because the lipase, which initially could decompose the ester bond portion of urethane and the MA ester which is the cross-linking sites in the hydrogel, became deactivated over time. Similarly, even though the PEU-MA hydrogels can be degraded at pH 4.0, the addition of H₂O₂ accelerated the degradation of the PEU-MA hydrogels over the first 5 days. The urethane, PEG and MA ester portions could be

decomposed by the hydroxyl radicals (\bullet OH). The degradation rate of the PEU2000-100MA gel was relatively faster than that of the PEU1000-100MA gel. This phenomenon can be explained by the different hydrophilicities and gel networks of the PEU1000-100MA and PEU2000-100MA gels. The strong hydrophobicity and high cross-linking density of the PEU1000-100MA gels result in a slow degradation.

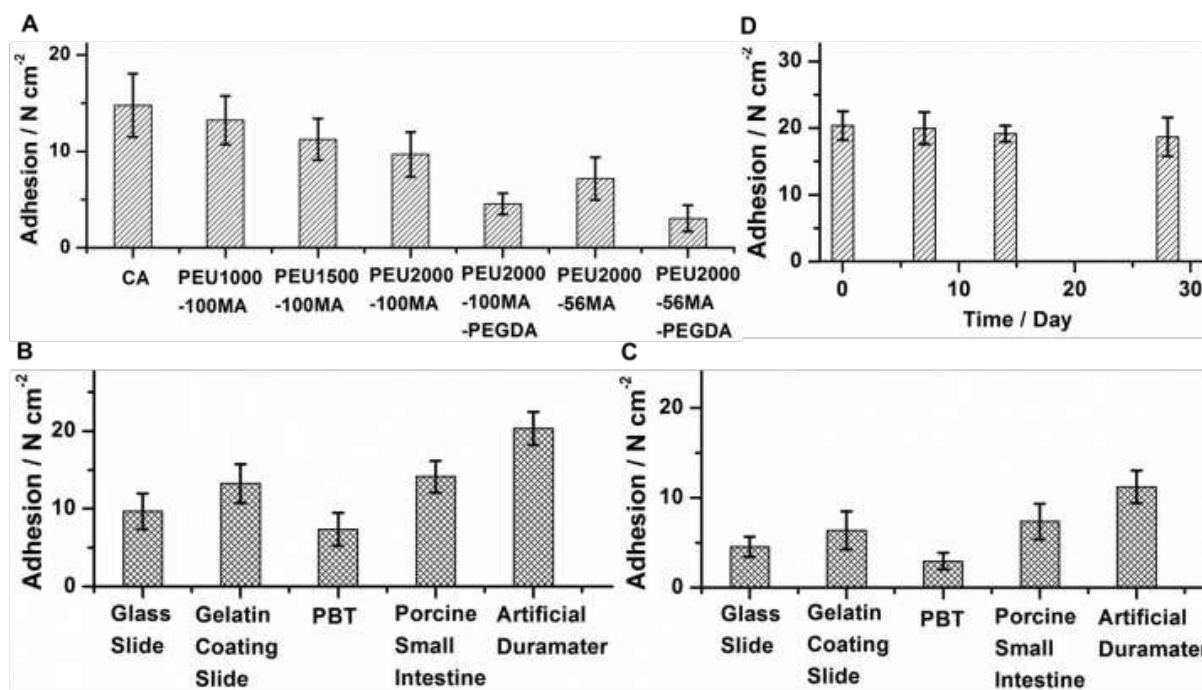


Figure 8. Tests of the adhesive strength of PEU-MA or PEU-MA-PEGDA gels. (A) Adhesions on the glass slide with different PEU hydrogels and medical-grade cyanoacrylate (CA); (B) Adhesions on different materials with PEU2000-100MA hydrogels; (C) Adhesions on different materials with PEU2000-100MA-PEGDA hydrogels; (D) Adhesions on artificial duramater with PEU2000-MA immersed in PBS of pH 7.4 at the time points of 0, 7, 14 and 28 days, 37 °C.

Moreover, the PEU-MA and PEU-MA-PEGDA gels with different grafting ratios of MA were degraded by ROS in the first 5 days. As shown in Fig. 6B, the degradation rate of PEU2000-56MA gels were faster than PEU2000-100MA gels, which could be explained by the lower cross-linking density of PEU2000-56MA gels than PEU2000-100MA gels. The lower of the grafting ratios of MA in PEU gels, the faster the degradation rates of the PEU gels were. However, the PEU2000-MA-PEGDA gels were degraded faster than PEU2000-MA gels at the same grafting ratios of MA. These phenomena were compared with the result of swelling test. Also, the cross-linking agent of PEGDA would be attacked by the hydroxyl radical.

In Vivo Mass Decrease of Gel Membranes. It has been demonstrated that the PEU-MA gel membranes could be degraded *in vitro* by lipase and ROS which were contained in the body. However, the concentrations of the lipase and ROS in the *in vitro* degradation experiments were much higher than which were contained *in vivo*. In order to study the *in vivo* degradability of photocured PEU-MA gels, the PEU2000-100MA and PEU2000-100MA-PEGDA gel membranes were selected as the samples to implant in the SD rats' subcutaneous

tissues. The mass decreases were detected at the time interval of 2, 4, 6 and 8 weeks after implantation. As shown Fig. 7, the remaining mass of PEU2000-100MA gel membrane was 74% for 8 weeks of implantation, and only 43% of PEU2000-100MA-PEGDA at the same time. It is predictable that these gel membranes could be completely degraded *in vivo* finally. The degradation rate of PEU2000-100MA was faster than PEU2000-100MA-PEGDA, which was similar to the phenomenon of *in vitro* degradation.

Adhesive Strength. The adhesive strength of PEU-MA and PEU-MA-PEGDA gels on different materials were summarized and shown in Fig. 8. As shown in Fig. 8A, the adhesions were decreased from PEU1000-100MA to PEU2000-100MA-PEGDA. The adhesion of PEU1000-100MA, PEU1500-100MA and PEU2000-100MA were 13.24, 11.26 and 9.68 N·cm⁻², respectively. These phenomena were related to the uniformity of the cross-linking point in the PEUs, which was compared with the results of swelling test. The adhesion of PEU2000-100MA was stronger than PEU2000-56MA owing to the lower cross-linking density of PEU2000-56MA gels than PEU2000-100MA gels, and the same to the PEU2000-100MA-PEGDA and PEU2000-56MA-PEGDA gels. However, the

adhesive strengths of PEU2000-MA-PEGDA were lower than the PEU2000-MA at the same grafting ratios of MA. These phenomena might indicate that the gel network formations of the PEU2000-MA are tighter than the PEU2000-MA-PEGDA.

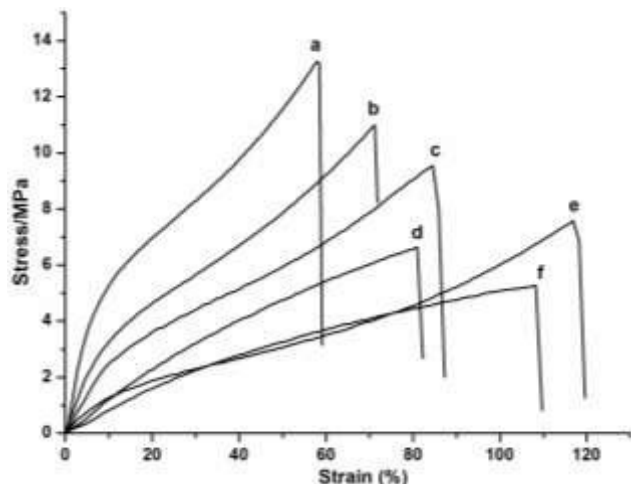


Figure 9. Stress-strain curves of the gel membranes of PEU1000-100MA (a), PEU1500-100MA (b), PEU2000-100MA (c), PEU2000-100MA-PEGDA (d), PEU2000-56MA (e) and PEU2000-56MA-PEGDA (f) at 25 °C, 200 mm min⁻¹.

Table 2. Tensile properties of PEU-MA and PEU-MA-PEGDA gel membranes

Gel Membranes	Young's Modulus (MPa)	Ultimate Strength (MPa)	Strain at Break (%)
PEU1000-100MA	70.12 ± 9.10	13.26 ± 3.18	57.9 ± 3.5
PEU1500-100MA	40.71 ± 5.26	10.99 ± 1.58	71.4 ± 6.3
PEU2000-100MA	25.46 ± 3.74	9.54 ± 2.10	84.9 ± 6.1
PEU2000-100MA-PEGDA	11.31 ± 1.32	6.61 ± 1.12	80.9 ± 5.4
PEU2000-56MA	15.18 ± 1.35	7.57 ± 1.12	116.9 ± 4.9
PEU2000-56MA-PEGDA	7.56 ± 0.71	5.23 ± 0.94	107.9 ± 6.9

All of the adhesions of the PEU gels are lower than CA, but the adhesions of dried PEU gels are stronger than CA (Fig. S13) except PEU2000-MA-PEGDA gels. As shown in Fig. 8B and 8C, the adhesions of PEU2000-100MA and PEU2000-100MA-PEGDA gels on the tissues (gelatin coating slide, porcine small intestine and artificial duramater) were stronger than on glass slide and PBT. The adhesion of PEU2000-100MA gels on artificial duramater was the strongest, which was as high as 20.35 N·cm⁻², and the PEU2000-100MA-PEGDA was 11.22 N·cm⁻². The adhesion of PEU gels on the tissues might be mainly caused by the hydrogen bond. As shown in Fig. 8D, the adhesions on the artificial duramater with PEU2000-100MA were not obviously decreased, which were immersed in PBS for 28 days. It was indicated that the PEU2000-100MA could well keep the adhesion on the tissues even when it was immersed in the water.

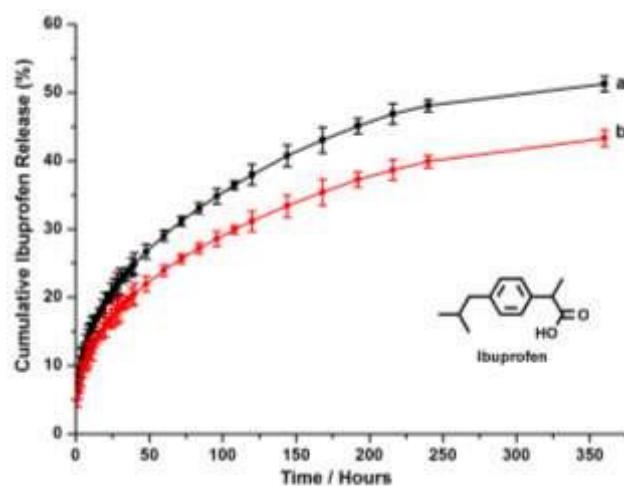


Figure 10. Ibuprofen release from photocured and ibuprofen-loaded PEU2000-100MA-PEGDA (a) and PEU2000-100MA (b) hydrogels at pH 7.4.

Tensile Properties. The tensile properties of the photocured PEU-MA and PEU-MA-PEGDA gel membranes which were dried under vacuum at 50 °C were studied with the tensile analysis at a strain rate of 200 mm·min⁻¹ at 25 °C. The stress-strain curves recorded by the tensile analyses are shown in Fig. 9, and the mechanical parameters are listed in Table 2. The stress-strain curves indicate that the PEG molecular weight has a significant influence on the mechanical properties of the materials. Lower PEG molecular weights lead to higher observed tensile strengths in the PEU-MA gel membranes. The Young's moduli of the PEU1000-100MA, PEU1500-100MA, and PEU2000-100MA gel membranes at the same grafting ratios of MA were found to be 70.12, 40.71 and 25.46 MPa, respectively. The strains at break of the PEU1000-100MA, PEU1500-100MA, and PEU2000-100MA gel membranes were 57.9%, 71.4%, and 84.9%, respectively. The results were compared with the swelling tests, which together showed that the cross-linking density of the PEU-MA gel membranes with short PEG molecular weights were tight at the same grafting ratios of MA. Moreover, the tensile strength was affected by the grafting ratios of MA of the gel membranes for the same PEU copolymer. The Young's moduli of the PEU2000-MA gel membranes at grafting ratios of MA of 100%, 56%, and 21% were found to be 25.46, 15.18 and 6.05 MPa, respectively, with strains at break of 84.9%, 116.9%, and 121.4%, respectively (Fig.S14).

Interestingly, the Young's moduli and strains at break of PEU2000-MA were both higher than the PEU2000-MA-PEGDA at the same grafting ratios of MA. And all the PEU-MA gel membranes (except PEU2000-21MA) were undergone a strain softening and then strain hardening procedure (Fig.8, a, b, c and e) during the tensile processes, which are different from the typical elastomers such as PEU2000-MA-PEGDA and PEU2000-21MA (Fig.8, d and f, and Fig S14). The strain softening of the PEU2000-MA might be caused by the dynamic recrystallization of the liner polymer chain in the gel membranes. And the strain hardening of the PEU2000-MA

might be caused by the formations of the cross-linking network. These results pointed toward that the PMA chains were formed when the MA moieties in PEU were reunited in the PEU2000-MA gels via the hydrophobic interactions. This leads to that the gel networks of PEU-MA are different from the typical cross-linking networks and are more like interpenetrating networks which contains the two networks of PEU and PMA (as shown in Fig. S15).^{71, 72} This analogously interpenetrating network leads to the high mechanical properties, strong adhesive strength, low swelling ratios and degradation rates of the PEU-MA gels. However, the grafting ratios of MA in PEU2000-21MA were so low that it was only formed the typical cross-linking networks (Fig. S14).

Study of Ibuprofen Release. If the PEU gels are used to the adhesive of subcutaneous tissue or visceral organ, the functional drugs could be loaded in the PEU-MA gels to achieve the outcome of anti-inflammatory and analgesia. In this study, ibuprofen was selected as a model drug for the drug release of PEU hydrogels owing to the UV-stability of ibuprofen. To evaluate the ability of the PEU hydrogels to effectively deliver ibuprofen, *in vitro* ibuprofen release from PEU2000-100MA and PEU2000-100MA-PEGDA gels (pH 7.4) at 37 °C was studied. Figure 10 shows the release profiles of ibuprofen from the PEU hydrogels. As shown in Fig. 10, about 51.3% of the ibuprofen was released from the ibuprofen-loaded PEU2000-100MA-PEGDA hydrogel, while about 43.3% of the ibuprofen was released from the PEU2000-100MA hydrogel over the tested 15 d period. These results indicate that the release of ibuprofen from ibuprofen-loaded PEU hydrogels is dependent on the network formations of PEU-MA and PEU-MA-PEGDA gels. The network formations of PEU2000-100MA are tighter than the cross-linking network formations PEU2000-100MA-PEGDA.

The release mechanism of ibuprofen from the degradable matrix is influenced both by diffusion of the drug and the degradation of the matrix,⁴³ although the PEU gels are degraded very slowly in PBS at pH 7.4. The Ritger-Peppas equation was used to study the mechanism of ibuprofen release from PEU2000-100MA and PEU2000-100MA-PEGDA hydrogels.⁷³ According to the Ritger-Peppas equation:

$$M_t / M_\infty = kt^n$$

where t refers to the drug release time, M_t / M_∞ is the drug fraction released at time t , and k and n are the constant and kinetic exponent of drug release, respectively. The n value calculated according to the equation for the initial several hours of PEU2000-100MA-PEGDA hydrogel was 0.412, indicating that the kinetics of ibuprofen release corresponds to that of typical Fickian diffusion, the same to the PEU2000-100MA gels of which the n value was 0.384. This phenomenon indicated that the PEU gels were difficult to degrade in the PBS at pH 7.4.

Cytotoxicity Evaluation. The cytotoxicity evaluation of the L-929 cells on the PEU-MA and PEU-MA-PEGDA gels were studied by examining the cell viability for 24 and 48 h with

MTT colorimetric assay. The positive control for this procedure was cells incubated in the complete medium but without the presence of the PEU-MA and PEU-MA-PEGDA gels. The relative cell viability on each PEU-MA or PEU-MA-PEGDA gel was examined in Fig. 11A. As shown in Fig. 11A, none of the gel groups showed cytotoxicity toward L-929 cells, and the cell viability of each gel was clearly increased from 24 to 48 h.

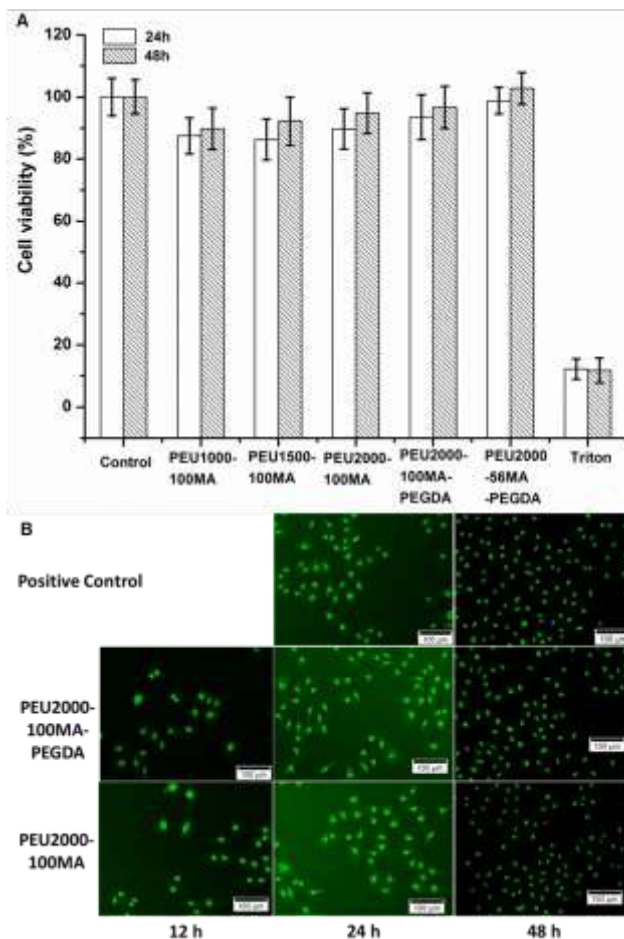


Figure 11. *In vitro* cytotoxicity of PEU-MA gels to NCTC clone 929 (L-929) cells following 24 and 48 h incubation (A) and Fluorescence images of L-929 cells cultured on the surface of photocured PEU2000-MA gels for 12, 24 and 48 hours. The cells were double stained with AO/EB. Scale bars = 100 μm (B).

In addition, after incubated with PEU2000-100MA-PEGDA and PEU2000-100MA gels for 12, 24 and 48 h, the L-929 cells were stained with acridine orange/ethidium bromide (AO/EB). The fluorescence micrographs were obtained with an inverted microscope to distinguish the living cells (green fluorescence) from the dead (red fluorescence). As can be observed in Fig. 11B, after a prolonged incubation time of 48 h, the cells treated with AO/EB staining present green fluorescence. Scarcely any red fluorescence could be seen in the micrographs on the surface of the PEU2000-MA and PEU2000-MA-PEGDA gels. This result indicates that the PEU2000-MA and PEU2000-MA-PEGDA hydrogel is conducive to cell growth and proliferation.

Conclusions

The temperature-sensitive PEU-MA copolymer hydrogels capable of chemically cross-linking were successfully synthesized based on PEU-MA copolymers. The PEU-MAs can be further cross-linked by photocuring after gelating at a specific temperature range. There are various advantages to these materials, including: (i) a rapid sol-gel phase transition via temperature response; (ii) the physical hydrogel can be further cross-linked by UV curing after temperature-sensitive gelating, and can keep its gel state and shape in a wide temperature range; (iii) the PEU-MA gels have high and persistent adhesive strength on the tissues especially on the artificial duramater and can load functional drugs; and (iv) the obtained gels have good mechanical property, biodegradability and biocompatibility. These materials show promise as biomaterials for tissue adhesive, especially for fixing and sealing the artificial duramater patches to prevent the leakage of cerebrospinal fluid. Thereinto, the PEU2000-100MA and PEU2000-100MA-PEGDA gels are most potentially applied to the tissue adhesive in clinical application due to their limited swelling ratios, excellent adhesive strength, and rapid gelation at the physiological temperature. These rapidly responsive and chemically crosslinkable hydrogels would be a promising candidate for rapid prototyping, and for filling or starting scaffolds that could be used for the loading drugs or growth factors to promote the repair and regeneration of soft tissues.

Acknowledgements

This work was funded by NSFC (51203079), the Natural Science Foundation of Tianjin (14JCYBJC18100), PCSIRT (IRT1257), and NFFTBS (J1103306).

Notes and references

^a Key Laboratory of Functional Polymer Materials of MOE, Institute of Polymers, Collaborative Innovation Centre of Chemical Science and Engineering (Tianjin), Nankai University, Tianjin 300071, PR China. Email: guolinwu@nankai.edu.cn; Fax: +86 22 23502749; Tel: +86 22 23507746

^b School of Chemistry and Chemical Engineering, Tianjin University of Technology, Tianjin 300191, PR China

† Footnotes should appear here. These might include comments relevant to but not central to the matter under discussion, limited experimental and spectral data, and crystallographic data.

Electronic Supplementary Information (ESI) available: [details of any supplementary information available should be included here]. See DOI: 10.1039/b000000x/

References

1. P. J. M. Bouten, M. Zonjee, J. Bender, S. T. K. Yauw, H. van Goor, J. C. M. van Hest and R. Hoogenboom, *Progress in Polymer Science*, 2014, **39**, 1375-1405.
2. A. L. Tajirian and D. J. Goldberg, *Journal of Cosmetic and Laser Therapy*, 2010, **12**, 296-302.
3. J. D. Lloyd, M. J. Marque, III and R. F. Kacprowicz, *Emergency Medicine Clinics of North America*, 2007, **25**, 73-+.
4. J. Bruce, Z. H. Krukowski, G. Al-Khairy, E. M. Russell and K. G. M. Park, *British Journal of Surgery*, 2001, **88**, 1157-1168.
5. J. Pickleman, W. Watson, J. Cunningham, S. G. Fisher and R. Gamelli, *Journal of the American College of Surgeons*, 1999, **188**, 473-482.
6. W. D. Spotnitz and S. Burks, *Clinical and Applied Thrombosis-Hemostasis*, 2010, **16**, 497-514.
7. W. D. Spotnitz and S. Burks, *Transfusion*, 2012, **52**, 2243-2255.
8. W. D. Spotnitz and S. Burks, *Transfusion*, 2008, **48**, 1502-1516.
9. D. M. Toriumi, W. F. Raslan, M. Friedman and M. E. Tardy, *Archives of otolaryngology--head & neck surgery*, 1990, **116**, 546-550.
10. A. Chow, H. Marshall, E. Zacharakis, P. Paraskeva and S. Purkayastha, *Journal of the American College of Surgeons*, 2010, **211**, 114-125.
11. P. Caliceti and F. M. Veronese, *Advanced Drug Delivery Reviews*, 2003, **55**, 1261-1277.
12. A. L. Klibanov, K. Maruyama, V. P. Torchilin and L. Huang, *FEBS Letters*, 1990, **268**, 235-237.
13. P. Ferreira, R. Pereira, J. F. J. Coelho, A. F. M. Silva and M. H. Gil, *International Journal of Biological Macromolecules*, 2007, **40**, 144-152.
14. P. Ferreira, J. F. J. Coelho and M. H. Gil, *International Journal of Pharmaceutics*, 2008, **352**, 172-181.
15. R. Jayakumar, M. Prabakaran, P. T. Sudheesh Kumar, S. V. Nair and H. Tamura, *Biotechnology Advances*, 2011, **29**, 322-337.
16. R. Jayakumar, D. Menon, K. Manzoor, S. V. Nair and H. Tamura, *Carbohydrate Polymers*, 2010, **82**, 227-232.
17. H. Tamura, T. Furuie, S. V. Nair and R. Jayakumar, *Carbohydrate Polymers*, 2011, **84**, 820-824.
18. M. Araki, H. Tao, N. Nakajima, H. Sugai, T. Sato, S.-H. Hyon, T. Nagayasu and T. Nakamura, *The Journal of Thoracic and Cardiovascular Surgery*, 2007, **134**, 1241-1248.
19. S. K. Bhatia, S. D. Arthur, H. K. Chenault, G. D. Figuly and G. K. Kodokian, *Current Eye Research*, 2007, **32**, 1045-1050.
20. K. A. Smeds, A. Pfister-Serres, D. L. Hatchell and M. W. Grinstaff, *Journal of Macromolecular Science-Pure and Applied Chemistry*, 1999, **A36**, 981-989.
21. K. A. Smeds and M. W. Grinstaff, *Journal of Biomedical Materials Research*, 2001, **54**, 115-121.
22. B. Petersen, A. Barkun, S. Carpenter, P. Chotiprasidhi, R. Chuttani, W. Silverman, N. Hussain, J. Liu, G. Taitelbaum and G. G. Ginsberg, *Gastrointestinal Endoscopy*, 2004, **60**, 327-333.
23. Z. Rao, M. Inoue, M. Matsuda and T. Taguchi, *Colloids and Surfaces B: Biointerfaces*, 2011, **82**, 196-202.
24. M. Matsuda, M. Ueno, Y. Endo, M. Inoue, M. Sasaki and T. Taguchi, *Colloids and Surfaces B: Biointerfaces*, 2012, **91**, 48-56.
25. E. Faure, C. Falentin-Daudré, C. Jérôme, J. Lyskawa, D. Fournier, P. Woisel and C. Detrembleur, *Progress in Polymer Science*, 2013, **38**, 236-270.
26. B. P. Lee, J. L. Dalsin and P. B. Messersmith, *Biomacromolecules*, 2002, **3**, 1038-1047.
27. T. W. Gilbert, S. F. Badylak, J. Gusenoff, E. J. Beckman, D. M. Clower, P. Daly and J. P. Rubin, *Plast Reconstr Surg*, 2008, **122**, 95-102.

28. N. Lang, M. J. Pereira, Y. Lee, I. Friehs, N. V. Vasilyev, E. N. Feins, K. Ablasser, E. D. O'Cearbhaill, C. Xu, A. Fabozzo, R. Padera, S. Wasserman, F. Freudenthal, L. S. Ferreira, R. Langer, J. M. Karp and P. J. del Nido, *Science Translational Medicine*, 2014, **6**.
29. E. Dolgin, *Nature Medicine*, 2013, **19**, 124-125.
30. W. D. Spotnitz, *American Surgeon*, 2012, **78**, 1305-1321.
31. C. M. Elvin, A. G. Brownlee, M. G. Huson, T. A. Tebb, M. Kim, R. E. Lyons, T. Vuocolo, N. E. Liyou, T. C. Hughes, J. A. M. Ramshaw and J. A. Werkmeister, *Biomaterials*, 2009, **30**, 2059-2065.
32. W. R. Ranger, D. Halpin, A. S. Sawhney, M. Lyman and J. Locicero, *The American surgeon*, 1997, **63**, 788-795.
33. A. C. O'Neill, J. M. Winograd, J. L. Zeballos, T. S. Johnson, M. A. Randolph, K. E. Bujold, I. E. Kochevar and R. W. Redmond, *Lasers in Surgery and Medicine*, 2007, **39**, 716-722.
34. A. Lauto, L. J. R. Foster, L. Ferris, A. Avolio, N. Zwaneveld and L. A. Poole-Warren, *Lasers in Surgery and Medicine*, 2004, **35**, 140-145.
35. P. Matteini, F. Ratto, F. Rossi and R. Pini, *Journal of Biomedical Optics*, 2012, **17**.
36. H. T. Spencer, J. T. Hsu, D. R. McDonald and L. I. Karlin, *Spine Journal*, 2012, **12**, E1-E6.
37. F. Fang, C. Gong, Z. Qian, X. Zhang, M. Gou, C. You, L. Zhou, J. Liu, Y. Zhang, G. Guo, Y. Gu, F. Luo, L. Chen, X. Zhao and Y. Wei, *Acs Nano*, 2009, **3**, 4080-4088.
38. C. Gong, B. Yang, Z. Qian, X. Zhao, Q. Wu, X. Qi, Y. Wang, G. Guo, B. Kan, F. Luo and Y. Wei, *Nanomedicine-Nanotechnology Biology and Medicine*, 2012, **8**, 963-973.
39. S. Z. Fu, Z. Li, J. M. Fan, X. H. Meng, K. Shi, Y. Qu, L. L. Yang, J. B. Wu, J. Fan, F. Luo and Z. Y. Qian, *Journal of Biomedical Nanotechnology*, 2014, **10**, 427-435.
40. V. M. Bispo, A. A. P. Mansur, E. F. Barbosa-Stancioli and H. S. Mansur, *Journal of Biomedical Nanotechnology*, 2010, **6**, 166-175.
41. L. Zhou, L. Yu, M. Ding, J. Li, H. Tan, Z. Wang and Q. Fu, *Macromolecules*, 2011, **44**, 857-864.
42. M. M. Ding, J. H. Li, H. Tan and Q. Fu, *Soft Matter*, 2012, **8**, 5414-5428.
43. X. Li, Y. Wang, J. Chen, Y. Wang, J. Ma and G. Wu, *ACS Applied Materials & Interfaces*, 2014, **6**, 3640-3647.
44. Y. Wang, X. Li, G. Wu, J. Chen, Y. Wang, H. Gao and J. Ma, *RSC Advances*, 2013, **3**, 13859-13868.
45. Y. Wang, G. Wu, X. Li, J. Chen, Y. Wang and J. Ma, *Journal of Materials Chemistry*, 2012, **22**, 25217-25226.
46. Y. Wang, G. Wu, X. Li, Y. Wang, H. Gao and J. Ma, *Biomaterials Science*, 2013, **1**, 614-624.
47. Y. Wang, G. Wu, X. Li, Y. Wang, H. Gao and J. Ma, *Journal of Biomaterials Science-Polymer Edition*, 2013, **24**, 1676-1691.
48. C. Pang, J. Zhang, G. Wu, Y. Wang, H. Gao and J. Ma, *Polymer Chemistry*, 2014, **5**, 2843-2853.
49. Z.-X. Jiang and Y. B. Yu, *Journal of Organic Chemistry*, 2007, **72**, 1464-1467.
50. M.-R. Park, C.-S. Cho and S.-C. Song, *Polymer Degradation and Stability*, 2010, **95**, 935-944.
51. B. J. Kim, D. X. Oh, S. Kim, J. H. Seo, D. S. Hwang, A. Masic, D. K. Han and H. J. Cha, *Biomacromolecules*, 2014, **15**, 1579-1585.
52. J. Wang, D. Zhao, Y. Wang and G. Wu, *RSC Advances*, 2014, **4**, 11244-11250.
53. J. Wang, C. Gong, Y. Wang and G. Wu, *RSC Advances*, 2014, **4**, 15856-15862.
54. C. Lu, B. Li, N. Liu, G. Wu, H. Gao and J. Ma, *RSC Advances*, 2014, **4**, 50301-50311.
55. W. Chen, F. Meng, F. Li, S.-J. Ji and Z. Zhong, *Biomacromolecules*, 2009, **10**, 1727-1735.
56. C. L. E. Nijst, J. P. Bruggeman, J. M. Karp, L. Ferreira, A. Zumbuehl, C. J. Bettinger and R. Langer, *Biomacromolecules*, 2007, **8**, 3067-3073.
57. T. Finkel and N. J. Holbrook, *Nature*, 2000, **408**, 239-247.
58. K. B. Beckman and B. N. Ames, *Physiological Reviews*, 1998, **78**, 547-581.
59. T. Nishikawa, D. Edelstein, X. L. Du, S. Yamagishi, T. Matsumura, Y. Kaneda, M. A. Yorek, D. Beebe, P. J. Oates, H. P. Hammes, I. Giardino and M. Brownlee, *Nature*, 2000, **404**, 787-790.
60. M. K. Chourasia and S. K. Jain, *Journal of Pharmacy and Pharmaceutical Sciences*, 2003, **6**, 33-66.
61. A. Bigi, G. Cojazzi, S. Panzavolta, K. Rubini and N. Roveri, *Biomaterials*, 2001, **22**, 763-768.
62. T. Nakaji-Hirabayashi, K. Kato and H. Iwata, *Biomaterials*, 2009, **30**, 4581-4589.
63. R. Chapanian, M. Y. Tse, S. C. Pang and B. G. Amsden, *Biomaterials*, 2009, **30**, 295-306.
64. H.-H. Chang, M.-C. Chang, L.-D. Lin, J.-J. Lee, T.-M. Wang, C.-H. Huang, T.-T. Yang, H.-J. Lin and J.-H. Jeng, *Biomaterials*, 2010, **31**, 6917-6925.
65. E. M. Christenson, M. Dadsetan, M. Wiggins, J. M. Anderson and A. Hiltner, *Journal of Biomedical Materials Research Part A*, 2004, **69A**, 407-416.
66. S. Krifka, G. Spagnuolo, G. Schmalz and H. Schweikl, *Biomaterials*, 2013, **34**, 4555-4563.
67. Y. Nobuhiko, O. Teruo and S. Yasuhisa, *J Control Release*, 1992, **22**, 105-116.
68. A. Farahnaky, D. A. Gray, J. R. Mitchell and S. E. Hill, *Food Hydrocolloids*, 2003, **17**, 321-326.
69. J. Tian, D. M. Peehl and S. J. Knox, *Cancer Biotherapy and Radiopharmaceuticals*, 2010, **25**, 439-448.
70. L.-P. Zhang, B. Hu and J.-H. Wang, *Analytica Chimica Acta*, 2012, **717**, 127-133.
71. J. P. Fouassier and J. Lalevee, *Polymers*, 2014, **6**, 2588-2610.
72. S. R. Batten and R. Robson, *Angewandte Chemie-International Edition*, 1998, **37**, 1460-1494.
73. P. L. Ritger and N. A. Peppas, *Journal of Controlled Release*, 1987, **5**, 37-42.